

Targeting the protein prenyltransferases efficiently reduces tumor development in mice with K-RAS-induced lung cancer

Meng Liu^{a,b,1}, Anna-Karin M. Sjögren^{a,1}, Christin Karlsson^a, Mohamed X. Ibrahim^a, Karin M. E. Andersson^a, Frida J. Olofsson^a, Annika M. Wahlstrom^a, Martin Dalin^a, Huiming Yu^b, Zhenggang Chen^{a,b}, Shao H. Yang^c, Stephen G. Young^c, and Martin O. Bergo^{a,2}

^aWallenberg Laboratory, Institute of Medicine, Sahlgrenska University Hospital, S-41345 Gothenburg, Sweden; ^bDepartment of Neurosurgery, Qilu Hospital, Shandong University, Jinan 250012, China; and ^cDepartments of Medicine and Human Genetics, David Geffen School of Medicine, University of California, Los Angeles, CA 90095

Edited by Tyler Jacks, Massachusetts Institute of Technology, Cambridge, MA, and approved March 3, 2010 (received for review July 25, 2009)

RAS and RHO proteins, which contribute to tumorigenesis and metastasis, undergo posttranslational modification with an isoprenyl lipid by protein farnesyltransferase (FTase) or protein geranylgeranyltransferase-I (GGTase-I). Inhibitors of FTase and GGTase-I were developed to block RAS-induced malignancies, but their utility has been difficult to evaluate because of off-target effects, drug resistance, and toxicity. Moreover, the impact of FTase deficiency and combined FTase/ GGTase-I deficiency has not been evaluated with genetic approaches. We found that inactivation of FTase eliminated farnesylation of HDJ2 and H-RAS, prevented H-RAS targeting to the plasma membrane, and blocked proliferation of primary and K-RAS^{G12D}-expressing fibroblasts. FTase inactivation in mice with K-RAS-induced lung cancer reduced tumor growth and improved survival, similar to results obtained previously with inactivation of GGTase-I. Simultaneous inactivation of FTase and GGTase-I markedly reduced lung tumors and improved survival without apparent pulmonary toxicity. These data shed light on the biochemical and therapeutic importance of FTase and suggest that simultaneous inhibition of FTase and GGTase-I could be useful in cancer therapeutics.

mouse models | non-small-cell lung cancer | protein farnesyltransferase | protein geranylgeranyltransferase type I

Many intracellular proteins, such as the RAS and RHO family proteins, are posttranslationally lipidated at a carboxyl-terminal *CAAX* motif. This process is called isoprenylation and is carried out by a pair of cytosolic enzymes, protein farnesyltransferase (FTase) and protein geranylgeranyltransferase type I (GGTase-I) (1). FTase and GGTase-I share a common α -subunit but have unique β -subunits that determine substrate specificity (2, 3). Some *CAAX* proteins, such as H-RAS, HDJ2, and prelamin A, are substrates for FTase, whereas others, such as RAPIA and RHOA, are substrates for GGTase-I (3). Protein isoprenylation facilitates membrane interactions, promotes protein–protein interactions, and can affect protein turnover (4).

The RAS proteins, by far the most thoroughly studied *CAAX* proteins, are involved in the pathogenesis of many forms of cancer (5). Because isoprenylation is essential for the plasma membrane targeting of the RAS proteins and their ability to transform cells (4), FTase inhibitors (FTIs) have been developed and tested as anticancer agents (6). FTIs showed efficacy in preclinical studies of malignancies, including those without RAS mutations (7–9). However, clinical trials of FTIs in humans have not been particularly successful (6). The mechanism by which FTIs inhibit cell growth is not entirely clear, but it likely involves interfering with the farnesylation of several *CAAX* proteins, in addition to RAS (6, 10, 11). Also, different FTIs have different properties (12–15), complicating efforts to define compound- versus mechanism-related effects.

A few years ago, Mijimolle et al. (16) attempted to address the functional relevance of FTase by generating mice with a conditional knockout allele for the gene encoding the β -subunit of FTase (*Fntb*). *Cre*-mediated recombination appeared to inhibit the farnesylation

of HDJ2 and H-RAS, but only partially, and, most remarkably, H-RAS remained in the membrane fraction of cells. They also reported that *Fntb*-deficient fibroblasts grew in culture and that the development of K-RAS-induced tumors was unaffected by *Fntb* deficiency. These findings were surprising for several reasons. First, FTI treatment studies had suggested that the membrane association of H-RAS is utterly dependent on protein farnesylation (17). Second, a nonprenylated mutant of H-RAS (C186S) is found exclusively in the soluble, cytosolic fraction of cells (18). Third, FTI treatment of cells typically results in cell-cycle arrest (19, 20). Fourth, in mouse models, FTIs are efficacious against many tumors, including those without RAS mutations (9, 21).

A potential explanation for the differences between the genetic and pharmacologic studies is that FTIs might affect other proteins aside from FTase. Another is that the *Fntb* knockout allele generated by Mijimolle et al. (16) yielded a transcript with an in-frame deletion (22), and it is conceivable that this mutant transcript yielded a protein with some residual enzymatic activity.

In FTI-treated cells, K-RAS and N-RAS are alternately prenylated by GGTase-I (23–25). That finding prompted both pharmaceutical companies and academic laboratories to develop GGTase-I inhibitors (GGTIs) (26), which have shown promise in preclinical studies (27–31). The rationale for inhibiting GGTase-I is supported by genetic studies in mice: Inactivating the gene for the β -subunit of GGTase-I (*Pggt1b*) reduced tumor formation and prolonged survival in mice with K-RAS-induced lung cancer (32).

Because neither an FTI alone nor a GGTI alone inhibits the prenylation of K- and N-RAS, FTI/GGTI combinations and dual-prenylation inhibitors (DPIs) were developed (33, 34). DPIs and FTI/GGTI combinations block K-RAS prenylation in vivo, but only at high doses that are toxic in mice. However, some studies with FTI/GGTI combinations did not report significant toxicity (27, 35). Thus far, no one has used genetic approaches to study dual inhibition of FTase and GGTase-I.

In this study, we created a conditional knockout allele for *Fntb* and reevaluated the impact of *Fntb* deficiency on protein isoprenylation, cell proliferation, and the growth of K-RAS-induced tumors. We also bred mice homozygous for conditional knockout alleles in both *Fntb* and *Pggt1b* and assessed the effect of combined FTase/GGTase-I deficiency on the development of K-RAS-induced lung cancer.

Author contributions: M.L., A.-K.M.S., S.G.Y., and M.O.B. designed research; M.L., A.-K.M.S., C.K., M.X.I., K.M.E.A., F.J.O., A.M.W., M.D., H.Y., Z.C., and S.H.Y. performed research; M.L., A.-K.M.S., and M.O.B. analyzed data; and M.L., A.-K.M.S., S.G.Y., and M.O.B. wrote the paper.

The authors declare no conflict of interest.

This article is a PNAS Direct Submission.

¹M.L. and A.-K.M.S. contributed equally to this work.

²To whom correspondence should be addressed. E-mail: martin.bergo@wlab.gu.se.

This article contains supporting information online at www.pnas.org/cgi/content/full/0908396107/DCSupplemental.

Results

Generation and Validation of a Conditional FTase Knockout Allele. To create a conditional knockout allele ($Fntb^{fl}$) for the β -subunit of FTase, we introduced *loxP* sites 1 kb upstream and 1 kb downstream of exon 1 (Fig. 1A). Mice homozygous for the conditional allele ($Fntb^{fl/fl}$) were healthy and fertile. $Fntb^{fl/fl}$ mice were bred first with EIIa-Cre mice (36) to remove a floxed *neo* cassette and then with deleter-Cre mice (37) to produce mice harboring one conditional knockout allele and one knockout allele ($Fntb^{fl/\Delta}$). Primary fibroblasts were cultured from E13.5 $Fntb^{fl/fl}$ embryos. When these cells were incubated with Cre-adenovirus (*adCre*), they were converted to $Fntb^{\Delta/\Delta}$ derivatives that had no detectable *Fntb* expression (Fig. 1B).

To assess the impact of *Fntb* deficiency on the isoprenylation of FTase substrates, we performed western blots of lysates from β -gal adenovirus- (*ad β gal*) and *adCre*-treated $Fntb^{fl/\Delta}$ fibroblasts and control fibroblasts ($Fntb^{fl/+}$). HDJ2 and H-RAS in extracts of *adCre*-treated $Fntb^{fl/\Delta}$ cells exhibited reduced electrophoretic mobilities (Fig. 1C), characteristic of the nonfarnesylated forms of these proteins. The absolute levels of HDJ2 did not change, but the levels of H-RAS in *adCre*-treated $Fntb^{fl/\Delta}$ cells were 2- to 4-fold higher than in control cells, as judged by densitometry (Fig. 1C).

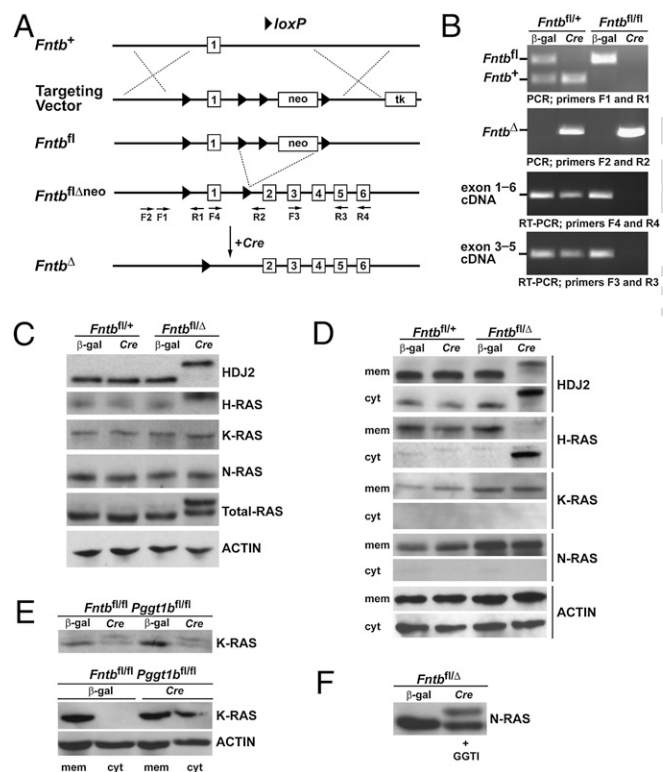


Fig. 1. A conditional knockout allele for the β -subunit of FTase ($Fntb^{fl}$). (A) Schematic of the *Fntb* gene-targeting vector. *LoxP* sites were inserted 1 kb upstream and downstream of exon 1. Arrows show the locations of primers for genotyping. *neo*, neomycin-resistance cassette; *tk*, thymidine kinase cassette. (B) PCR and RT-PCR analyses demonstrating the inactivation of *Fntb* by treatment with *adCre*. $Fntb^{fl/+}$ and $Fntb^{fl/fl}$ fibroblasts were incubated with *ad β gal* or *adCre*, and genomic DNA and total RNA were isolated 4 days later. (C) Western blots of extracts from $Fntb^{fl/+}$ and $Fntb^{fl/\Delta}$ fibroblasts incubated with *ad β gal* or *adCre*. An antibody against actin was used as a loading control. (D) Western blots showing the distribution of proteins in the membrane (mem) and cytosolic (cyt) fractions of *ad β gal*- or *adCre*-treated fibroblasts. (E) (Upper) K-RAS western blot of extracts from $Fntb^{fl/fl}$ $Pggt1b^{fl/fl}$ fibroblasts that had been incubated with *ad β gal* or *adCre*. (Lower) Western blot showing the distribution of K-RAS in the membrane and cytosolic fractions of $Fntb^{fl/fl}$ $Pggt1b^{fl/fl}$ fibroblasts incubated with *ad β gal* or *adCre*. (F) N-RAS western blot of $Fntb^{fl/\Delta}$ fibroblasts treated with *adCre* and 10 μ M GGTI for 4 days.

The electrophoretic mobilities of K-RAS and N-RAS were unchanged, likely because these proteins are isoprenylated by GGTase-I (23–25). HDJ2 and H-RAS accumulated in the cytosolic fraction of $Fntb^{\Delta/\Delta}$ cells, whereas K- and N-RAS remained associated with the membrane fraction (Fig. 1D). Inactivating a single *Fntb* allele in $Fntb^{fl/+}$ fibroblasts with *adCre* did not affect the electrophoretic mobilities or the membrane/cytosolic partitioning of HDJ2 and H-RAS (Fig. 1C and D).

To determine whether K-RAS and N-RAS are geranylgeranylated in $Fntb^{\Delta/\Delta}$ cells, we isolated $Fntb^{fl/fl}$ $Pggt1b^{fl/fl}$ fibroblasts and treated them with *adCre* to inactivate both *Fntb* and *Pggt1b* ($Fntb^{\Delta/\Delta}$ $Pggt1b^{\Delta/\Delta}$). In $Fntb^{\Delta/\Delta}$ $Pggt1b^{\Delta/\Delta}$ cells, a substantial proportion of K-RAS accumulated in the cytosolic fraction and exhibited a reduced electrophoretic mobility (Fig. 1E). A similar shift in the mobility of N-RAS was observed in $Fntb^{\Delta/\Delta}$ cells treated with a GGTI (Fig. 1F). $Fntb^{\Delta/\Delta}$ $Pggt1b^{\Delta/\Delta}$ cells remained viable for a few days, but they underwent apoptosis and died within 4 days (Fig. S1A and B). Inactivating *Fntb* and *Pggt1b* in cells expressing oncogenic H-RAS targeted to the plasma membrane by an amino-terminal myristoylation sequence also underwent apoptosis (Fig. S1C and D).

***Fntb* Deficiency Blocks Proliferation of Primary and K-RAS^{G12D}-Expressing Fibroblasts.** Inactivating a single *Fntb* allele in $Fntb^{fl/+}$ fibroblasts with *adCre* did not affect cell proliferation (Fig. 2A). However, inactivating both alleles by treating primary $Fntb^{fl/\Delta}$ fibroblasts with *adCre* dramatically reduced proliferation (Fig. 2A). Similar results were found with primary and immortalized $Fntb^{fl/fl}$ cells. Genotypically confirmed $Fntb^{\Delta/\Delta}$ fibroblasts were large and flat and accumulated in the G₂M phase of the cell cycle (Fig. 2B and C), but the number of apoptotic cells was low (Fig. S1A). Inactivating *Fntb* in primary fibroblasts increased p21^{CIP1} levels and delayed serum-stimulated phosphorylation of AKT but did not affect levels of phosphorylated MEK and ERK1/2 (Fig. S2).

When *adCre*-treated $Fntb^{fl/fl}$ cells were left on the culture plates for more than a week, cell growth gradually resumed. However, this growth was due to overgrowth by $Fntb^{fl/\Delta}$ cells (rather than $Fntb^{\Delta/\Delta}$ cells) (Fig. 2D). Despite extensive efforts, we were unable to clone $Fntb^{\Delta/\Delta}$ fibroblasts from *adCre*-treated $Fntb^{fl/fl}$ cells. In more than 12 independent experiments, cell growth late after *adCre* treatment was invariably due to overgrowth by $Fntb^{fl/\Delta}$ cells (Fig. 2E). In contrast, we had no difficulty in obtaining stable $Fntb^{\Delta/+}$ cell lines after treating $Fntb^{fl/+}$ cells with *adCre* (Fig. 2E).

To assess the impact of *Fntb* deficiency on the proliferation of cells expressing K-RAS^{G12D}, we isolated primary fibroblasts from $Fntb^{fl/\Delta}$ and $Fntb^{fl/+}$ embryos harboring an inducible oncogenic K-RAS allele (K^{LSL}) (38). The K^{LSL} allele is normally silent but K-RAS^{G12D} expression can be induced with *Cre*. Incubation of $Fntb^{fl/+}$ K^{LSL} fibroblasts with *adCre* yielded $Fntb^{\Delta/+}$ K^{G12D} cells that proliferated more rapidly (Fig. 2F). In contrast, *adCre* treatment of $Fntb^{fl/\Delta}$ K^{LSL} cells (producing $Fntb^{\Delta/\Delta}$ K^{G12D} cells) resulted in G₂M cell-cycle arrest (Fig. 2F and G).

Inactivating *Fntb* Increases Survival of Mice with K-RAS-Induced Lung Cancer. To determine the effect of an *Fntb* knockout on the development of a K-RAS-induced malignancy, we bred mice carrying the K^{LSL} allele (*K*) and a lysozyme M-Cre allele (*L*) on $Fntb^{fl/\Delta}$ and $Fntb^{fl/+}$ backgrounds (mice harboring both alleles were designated *KL*). Littermate $Fntb^{fl/\Delta}$ *L* mice were monitored to assess the impact of *Fntb* deficiency in the absence of K-RAS-induced tumors; $Fntb^{fl/+}$ *L*, $Fntb^{fl/+}$ *K*, and $Fntb^{fl/\Delta}$ *K* mice were used as healthy controls (*Ctrl* mice).

We previously showed that *KL* mice express K-RAS^{G12D} in most or all type II pneumocytes and develop lung cancer that is fatal by 25 days of age. Lung weight is increased ~10-fold and alveoli are obliterated by diffuse hyperplasia and adenocarcinoma (32). In keeping with those findings, the maximum survival of $Fntb^{fl/+}$ *KL* mice was 24 days (Fig. 3A). The survival of $Fntb^{fl/\Delta}$ *KL* mice was

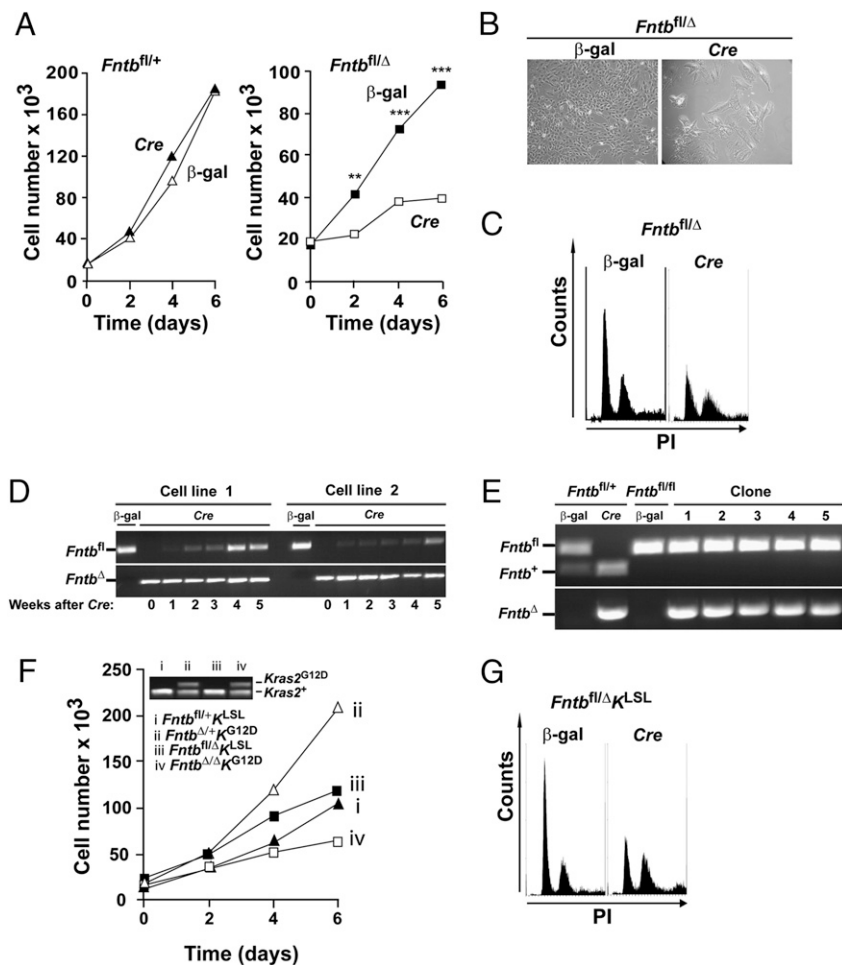


Fig. 2. Inactivating *Fntb* stops fibroblast proliferation. (A) Proliferation of *Fntb*^{fl/+} and *Fntb*^{fl/Δ} primary mouse fibroblasts incubated with *adβgal* or *adCre*. Data show a single cell line assayed in triplicate. Similar results were obtained with two different cell lines of each genotype. ***P* < 0.01; ****P* < 0.001. (B) Photomicrographs of *Fntb*^{fl/Δ} cells incubated with *adβgal* or *adCre*. (C) Cell-cycle analysis of *Fntb*^{fl/Δ} fibroblasts incubated with *adβgal* or *adCre*. PI, propidium iodide. (D) PCR genotyping of genomic DNA from *Fntb*^{fl/+} fibroblasts at various times after incubation with *adβgal* or *adCre*. (E) PCR genotyping of genomic DNA from individual clones of *adβgal*- or *adCre*-treated *Fntb*^{fl/+} and *Fntb*^{fl/Δ} fibroblasts. (F) Proliferation of primary *Fntb*^{fl/+}*K*^{LSL} and *Fntb*^{fl/Δ}*K*^{LSL} fibroblasts incubated with *adβgal* or *adCre*. Data represent the mean of a single cell line/genotype assayed in triplicate. Similar results were obtained in two independent experiments with two cell lines/genotypes. Inset shows PCR genotyping of genomic DNA demonstrating the activation of the *K*^{G12D} allele in cells incubated with *adCre* (ii and iv) but not in cells incubated with *adβgal* (i and iii). (G) Cell-cycle analysis of *adβgal*- and *adCre*-treated *Fntb*^{fl/Δ}*K*^{LSL} fibroblasts. The experiment was repeated three times with similar results.

significantly longer, >100 days in some cases (*P* < 0.0001; Fig. 3A). The lung weights in 3-week-old *Fntb*^{fl/Δ}*KL* mice were lower than in *Fntb*^{fl/+}*KL* mice (*P* < 0.0001) but higher than in *Fntb*^{fl/Δ}*L* mice or *Ctrl* mice (Fig. 3B). Moreover, histologic analyses revealed nearly complete obliteration of alveoli in *Fntb*^{fl/+}*KL* lungs, whereas *Fntb*^{fl/Δ}*KL* lungs retained areas of normal histology (Fig. 3C). Survival, lung weight, and lung histology in *Fntb*^{fl/Δ}*L* mice were indistinguishable from those of *Ctrl* mice (Fig. 3A–C).

PCR genotyping of genomic DNA from *Fntb*^{fl/Δ}*KL* lungs revealed activation of the K-RAS^{G12D} allele and a recombined *Fntb* allele (Fig. 3D). We harvested protein lysates from lung tissue from 3-week-old *Fntb*^{fl/+}*KL* and *Fntb*^{fl/Δ}*KL* mice and performed western blots with antibodies against the CAAX proteins, H-RAS, HDJ2, and prelamin A, which serve as markers of cellular FTase activity (39). In lung extracts of *Fntb*^{fl/Δ}*KL* mice, a substantial proportion of H-RAS accumulated in the cytosolic fraction, whereas K-RAS remained in the membrane fraction (Fig. 3E). Approximately 50% of the HDJ2 in *Fntb*^{fl/Δ}*KL* lungs exhibited a reduced electrophoretic mobility (Fig. 3F). Also, reduced FTase activity resulted in an accumulation of nonfarnesylated prelamin A (Fig. 3F). There was no difference in levels of phosphorylated ERK1/2 in lung extracts from *Fntb*^{fl/+}*KL* and *Fntb*^{fl/Δ}*KL* lungs (Fig. 3F).

Simultaneous Inactivation of *Fntb* and *Pggt1b* Reduces Tumor Load. To assess the effect of combined *Fntb* and *Pggt1b* deficiency on K-RAS-induced tumors, we bred *Fntb*^{fl/Δ}*Pggt1b*^{fl/Δ}*KL* mice and control *KL* mice in which neither prenyltransferase was inactivated. Littermate *Fntb*^{fl/+}*Pggt1b*^{fl/Δ}*L* mice were analyzed to determine the impact of *Fntb*/*Pggt1b* deficiency in the absence of K-

RAS-induced tumors. *Fntb*^{fl/+}*Pggt1b*^{fl/+}*L*, *Fntb*^{fl/Δ}*Pggt1b*^{fl/+}*L*, and *Fntb*^{fl/+}*Pggt1b*^{fl/Δ}*L* mice (collectively designated *Ctrl*) were used as healthy controls.

Lung weight and histology were indistinguishable in 3-week-old *Fntb*^{fl/Δ}*Pggt1b*^{fl/Δ}*KL* and *Ctrl* mice (Fig. 4A and B). But in 3-week-old *KL* mice, lung weight was 10-fold higher than in *Ctrl* mice (as a result of tumor burden), and the maximum survival was 24 days (Fig. 4A–C). The levels of phosphorylated ERK1/2 in lung lysates were lower in *Fntb*^{fl/Δ}*Pggt1b*^{fl/Δ}*KL* mice than in *KL* mice (Fig. 4D), as were K_i-67 levels (as judged by immunofluorescence confocal microscopy) (Fig. 4E). *Fntb*^{fl/Δ}*Pggt1b*^{fl/Δ}*KL* mice survived far longer than *KL* mice (median, 170 vs. 22 days; *P* < 0.0001) (Fig. 4C), but all eventually developed tumors and were euthanized. Lung histology and survival were indistinguishable in *Fntb*^{fl/Δ}*Pggt1b*^{fl/Δ}*L* and *Ctrl* mice (Fig. 4B and C).

To determine whether farnesylation and geranylgeranylation were inhibited in lungs of *Fntb*^{fl/Δ}*Pggt1b*^{fl/Δ}*KL* mice, we performed western blots on lung lysates from 3-week-old mice. Approximately 25% of HDJ2 exhibited a reduced electrophoretic mobility, characteristic of the nonfarnesylated protein. Protein geranylgeranylation was also inhibited, as the nonprenylated (np) form of RAP1A accumulated in lung lysates (Fig. 5A). Moreover, a large proportion of K-RAS accumulated in the cytosolic fraction of lung lysates from *Fntb*^{fl/Δ}*Pggt1b*^{fl/Δ}*KL* mice, suggesting that many cells lacked both FTase and GGTase-I activity (Fig. 5B). Immunofluorescence and confocal microscopy revealed prelamin A staining in lung sections from *Fntb*^{fl/Δ}*KL* and *Fntb*^{fl/Δ}*Pggt1b*^{fl/Δ}*KL* mice, whereas np-RAP1A staining was detected only in the lungs of *Fntb*^{fl/Δ}*Pggt1b*^{fl/Δ}*KL* mice (Fig. 5C). Some cells in lungs from *Fntb*^{fl/Δ}*Pggt1b*^{fl/Δ}*KL* mice exhibited

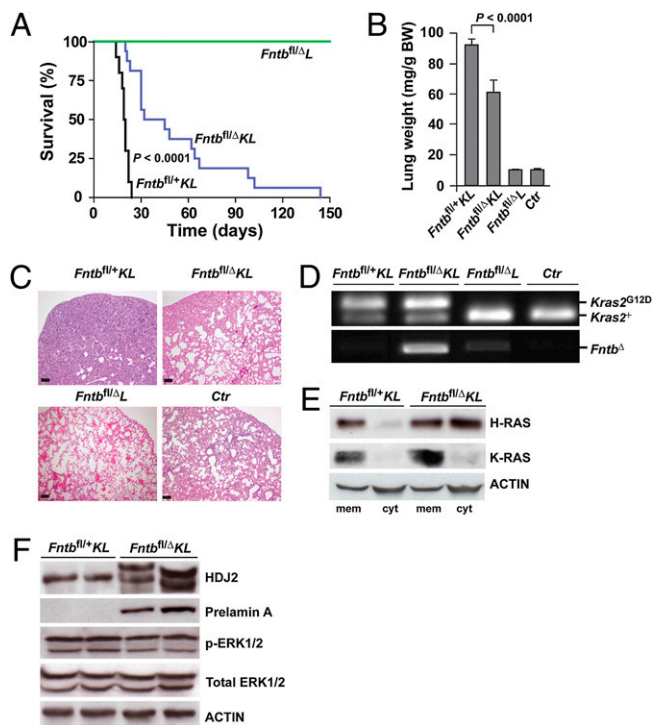


Fig. 3. Inactivation of *Fntb* reduces tumor development and prolongs survival of mice with K-RAS-induced lung cancer. (A) Kaplan–Meier curve showing increased survival in *Fntb*^{fl/Δ}KL mice (*n* = 16) compared with *Fntb*^{fl/*}KL mice (*n* = 10). All *Fntb*^{fl/Δ} mice (*n* = 9) were alive at the end of the experiment (150 days). (B) Lung weight in 3-week-old *Fntb*^{fl/*}KL (*n* = 8), *Fntb*^{fl/Δ}KL (*n* = 7), *Fntb*^{fl/Δ}L (*n* = 6), and *Ctrl* (*n* = 5) mice. (C) Hematoxylin/eosin-stained sections of lungs from 3-week-old mice. (Scale bars, 100 μm.) (D) Genotyping of wild-type and activated *K*^{G12D} alleles and the recombined *Fntb*^Δ allele by PCR amplification of genomic DNA from lung tissue. (E) Western blot showing the distribution of H-RAS and K-RAS in membrane and cytosolic fractions of lung lysates. (F) Western blots of protein lysates from the lungs of 3-week-old mice. Actin was used as a loading control.

strong staining for both prelamins A and np-RAP1A (Fig. 5C and Fig. S34). These double-positive cells were also identified in lungs of *Fntb*^{fl/Δ}*Pggt1b*^{fl/Δ} mice, and some of those cells were type II pneumocytes because they were also positive for SP-C (Fig. S3B). Moreover, K-RAS was identified in the cytosolic fraction of lung lysates from *Fntb*^{fl/Δ}*Pggt1b*^{fl/Δ} mice (Fig. S3C). Despite the presence of cells that apparently lacked both FTase and GGTase-I activity, we found

no evidence of apoptosis in lung sections of *Fntb*^{fl/Δ}*Pggt1b*^{fl/Δ}L mice (Fig. S4).

In the immunohistochemistry analyses, we detected cells in lungs of *Fntb*^{fl/Δ}*Pggt1b*^{fl/Δ}KL mice that were positive for np-RAP1A but not prelamins A (Fig. S34) and cells that were negative for both. We suspect that incomplete recombination in the *Fntb* and *Pggt1b* alleles underlies the development of tumors in older *Fntb*^{fl/Δ}*Pggt1b*^{fl/Δ}KL mice. Indeed, the percentage of genomic DNA with an inactivated *Fntb* allele fell from 18% in 3-week-old mice to 5% in the tumors of 198-day-old mice. Simultaneously, the percent inactivation of the *Pggt1b* gene fell from 20% in 3-week-old mice to 10% in tumors of 198-day-old mice (Fig. 5D).

Simultaneous Inactivation of *Fntb* and *Pggt1b* Inhibits Tumorigenesis in a Second K-RAS-Induced Lung Tumor Model.

To further investigate how inactivating *Fntb* and *Pggt1b* affects tumor development, we administered *adCre* to *Fntb*^{fl/Δ}*Pggt1b*^{fl/Δ}K mice, *K* mice heterozygous for one or both of the conditional alleles, and healthy *Ctrl* mice (38). *AdCre* results in *K*^{G12D} expression in a limited number of cells, leading to a limited number of tumors that can be characterized in number, grade, and lesion area. Eight weeks after administration of 5×10^7 pfu *adCre*, *K* mice had large tumors that were easily visible on the surface of the lungs (Fig. 6A–C). However, the lung surface of *adCre*-treated *Fntb*^{fl/Δ}*Pggt1b*^{fl/Δ}K mice was nearly indistinguishable from that of *Ctrl* mice, and *Fntb*^{fl/Δ}*Pggt1b*^{fl/Δ}K mice had 76% fewer tumors and 79% smaller lesion area than *K* mice (Fig. 6A–C). The lung lesions in *K* mice ranged from atypical adenomatous hyperplasia and epithelial hyperplasia to adenocarcinoma, the most common lesion (identified in 7 of 8 mice; Fig. 6D). The lung histology of *Fntb*^{fl/Δ}*Pggt1b*^{fl/Δ}K mice ranged from entirely normal to the presence of epithelial hyperplasia (Fig. 6D) and small adenomas; adenocarcinoma was observed in only 1 of 11 mice.

Discussion

In this study, we produced mice with a conditional knockout allele for *Fntb* and showed that inactivation of *Fntb* eliminated farnesylation of HDJ2 and H-RAS, prevented membrane targeting of H-RAS, and blocked the proliferation of primary, immortalized, and K-RAS^{G12D}-expressing fibroblasts in vitro. Moreover, inactivating *Fntb* in mice with K-RAS-induced lung cancer reduced tumor growth and improved survival. In addition, simultaneous inactivation of *Fntb* and *Pggt1b* had a strong antitumor effect.

Our findings differ significantly from those of Mijimolle et al. (16). In the latter study, the *Fntb* knockout did not affect H-RAS membrane association or stop fibroblast proliferation, nor did it affect the development of K-RAS-induced tumors in mice. When their report was published, it was provocative because it challenged both the

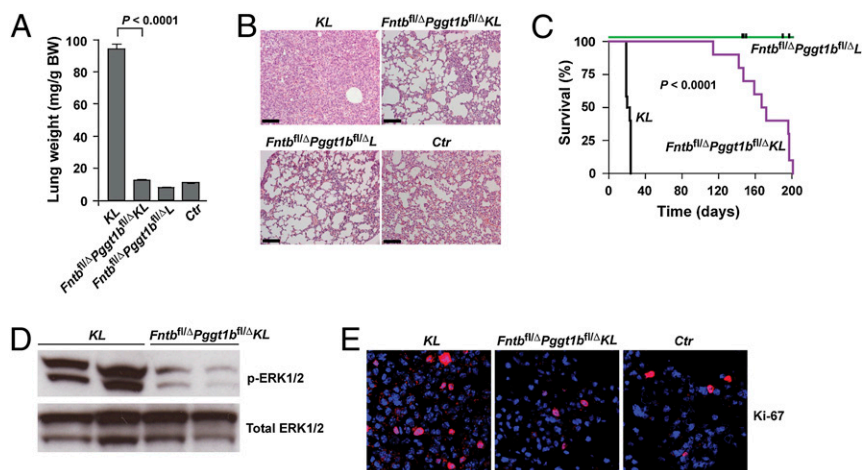


Fig. 4. Simultaneous inactivation of *Fntb* and *Pggt1b* in mice with K-RAS^{G12D}-induced lung cancer. (A) Lung weight of 3-week-old KL (*n* = 4), *Fntb*^{fl/Δ}*Pggt1b*^{fl/Δ}KL (*n* = 6), *Fntb*^{fl/Δ}*Pggt1b*^{fl/Δ}L (*n* = 5), and *Ctrl* (*n* = 9) mice. BW, body weight. (B) Representative hematoxylin/eosin-stained lung sections of mice from the experiment shown in A. (Scale bars, 100 μm.) (C) Kaplan–Meier curve showing survival of KL (*n* = 12), *Fntb*^{fl/Δ}*Pggt1b*^{fl/Δ}KL (*n* = 10), and *Fntb*^{fl/Δ}*Pggt1b*^{fl/Δ}L (*n* = 9) mice. Black tick marks indicate healthy *Fntb*^{fl/Δ}*Pggt1b*^{fl/Δ}L mice that were euthanized for tissue analyses. (D) Western blots of protein extracts from the lungs of 3-week-old KL and *Fntb*^{fl/Δ}*Pggt1b*^{fl/Δ}KL mice showing levels of phosphorylated ERK1/2. Total ERK1/2 was used as a loading control. (E) Confocal immunofluorescence micrographs showing expression of Ki-67 (pink) in cells from KL, *Fntb*^{fl/Δ}*Pggt1b*^{fl/Δ}KL, and *Ctrl* mice. Nuclei were visualized with DAPI (blue).

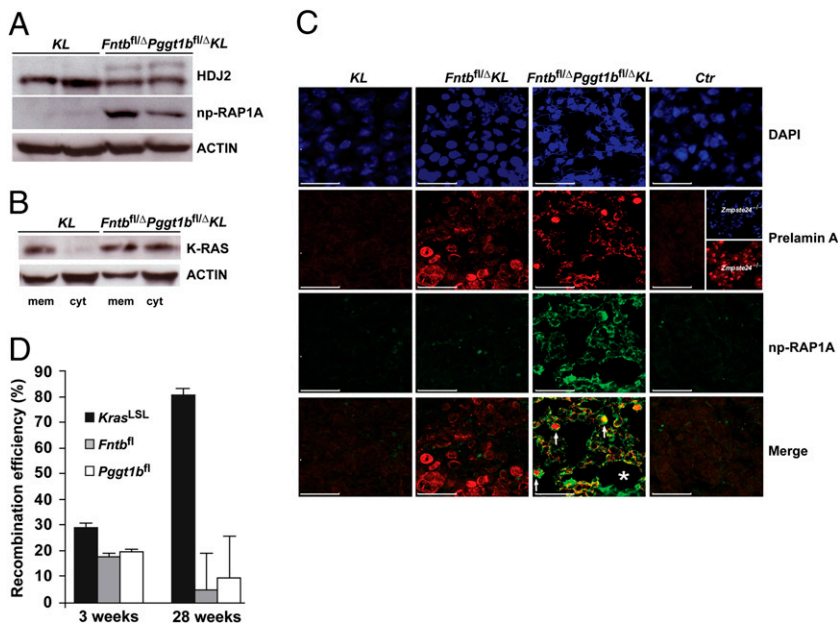


Fig. 5. Reduced FTase and GGTase-I activities in lungs of *Fntb^{fl/Δ}Pggt1b^{fl/Δ}KL* mice. (A) Western blots of protein extracts from lungs of 3-week-old *KL* and *Fntb^{fl/Δ}Pggt1b^{fl/Δ}KL* mice. Actin was used as a loading control. (B) Western blot showing the distribution of K-RAS in the membrane and cytosolic fractions of *KL* and *Fntb^{fl/Δ}Pggt1b^{fl/Δ}KL* mice. (C) Confocal immunofluorescence microscopy showing prelamin A (red) and np-RAP1A (green) expression in lung sections from 3-week-old *KL*, *Fntb^{fl/Δ}KL*, *Fntb^{fl/Δ}Pggt1b^{fl/Δ}KL*, and *Ctrl* mice. Nuclei were stained with DAPI (blue). The specificity of prelamin A staining was established with lung sections of *Zmpste24^{-/-}* mice (where prelamin A accumulates due to a defect in the conversion of farnesyl-prelamin A to mature lamin A). Arrows indicate cells positive for both prelamin A and np-RAP1A. Asterisk, alveolus. (Scale bars, 25 μ m.) (D) Recombination efficiency of the “floxed” *K^{LSL}*, *Fntb^{fl}*, and *Pggt1b^{fl}* alleles determined by quantitative PCR of genomic DNA from lung biopsies of 3-week-old *Fntb^{fl/Δ}Pggt1b^{fl/Δ}KL* mice ($n = 5$) and from lung tumors of 28-week-old *Fntb^{fl/Δ}Pggt1b^{fl/Δ}KL* mice ($n = 2$).

widely accepted notion that H-RAS association with membranes depends on protein farnesylation and the view that HDJ2 prenylation depends on FTase. The explanation for the differences between our studies and theirs is unknown; however, we suspect that the differences might relate to the fact that Mijimolle et al.’s allele yielded an unexpected splicing event. Rather than generating a transcript with a nonsense mutation, the mutation yielded a short in-frame deletion in the *Fntb* transcript (22). In contrast, the recombination event in our

Fntb allele deleted the promoter and exon 1 and created a bona fide null allele.

Inactivating *Fntb* in fibroblasts induced a G₂M arrest associated with large flattened cells, up-regulated p21^{CIP1}, and reduced serum-stimulated phosphorylation of AKT. Previously, we showed that inactivation of *Pggt1b* induces a G₁ arrest associated with cell rounding and up-regulation of p21^{CIP1}. The cell rounding and cell-cycle arrest could be overcome, at least temporarily, by expressing farnesylated mutants of RHOA and CDC42, suggesting that a limited number of geranylgeranylated proteins are important for those phenotypes. The creation of a bona fide knockout allele for the *Fntb* allele opens the door to performing similar experiments to determine whether geranylgeranylated versions of FTase substrates reverse the phenotypes of *Fntb*-deficient cells.

Fntb deficiency reduced tumor growth and improved survival in mice with K-RAS-induced lung cancer, similar to the effects of inactivating *Pggt1b* (32). Because K-RAS remains prenylated and associated with membranes in both *Fntb*- and *Pggt1b*-deficient cells, these studies support the notion (40) that the therapeutic effects of FTIs and GGTIs are independent of the RAS proteins.

We hypothesized that simultaneous inactivation of *Fntb* and *Pggt1b* would limit tumor growth more effectively than inactivation of either gene alone—in part because this approach would be predicted to inhibit K-RAS prenylation and membrane association. The simultaneous inactivation strategy was effective, at least to an extent, because a substantial proportion of K-RAS in lysates from *Fntb/Pggt1b*-deficient fibroblasts, lung tissue, and lung tumors accumulated in the cytosolic fraction. As we predicted, the simultaneous inactivation of *Fntb* and *Pggt1b* had a far greater inhibitory effect on K-RAS-induced tumors than inactivation of either gene alone. However, the main effect of inhibiting FTase and GGTase-I is likely independent of the RAS proteins because both control and myristoylated H-RAS-transfected fibroblasts underwent apoptosis after inactivation of both *Fntb* and *Pggt1b*.

The main concern surrounding the combined inhibition of FTase and GGTase-I has been toxicity (33, 34). Whereas the simultaneous inactivation of *Fntb* and *Pggt1b* clearly induced cell death in fibroblasts, the inactivation of both genes in type II pneumocytes in *Fntb^{fl/Δ}Pggt1b^{fl/Δ}L* mice did not produce pulmonary disease phenotypes and did not induce apoptosis. Moreover, *Fntb^{fl/Δ}Pggt1b^{fl/Δ}KL* mice appeared healthy for several months despite widespread expression of K-RAS^{G12D} in the lung. Some

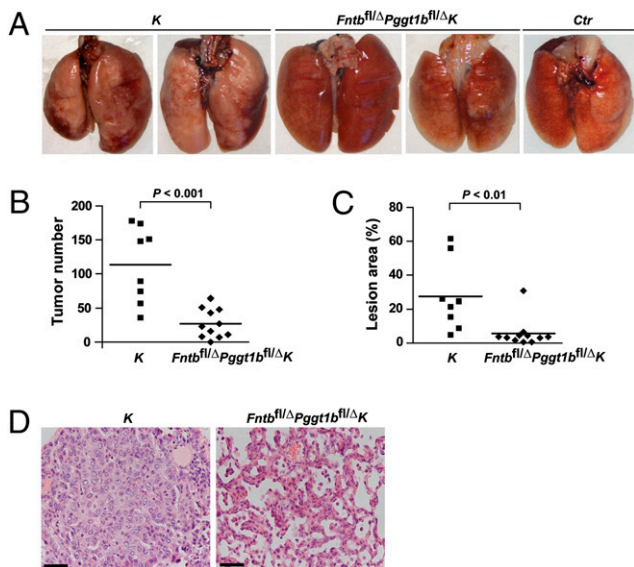


Fig. 6. Inactivation of *Fntb* and *Pggt1b* reduces tumor burden in a second K-RAS^{G12D}-induced lung cancer model. (A) Photographs of lungs 8 weeks after inhalation of *adCre*. Note the extensive lesions (white areas) on the surface of lungs from *K* mice and the relatively normal appearance of the lungs from *Fntb^{fl/Δ}Pggt1b^{fl/Δ}K* mice. (B and C) Tumor number (B) and surface area (C) in lungs from *K* ($n = 8$) and *Fntb^{fl/Δ}Pggt1b^{fl/Δ}K* ($n = 11$) mice 8 weeks after inhalation of *adCre*. (D) Hematoxylin/eosin-stained sections of typical lesions in lungs from *K* and *Fntb^{fl/Δ}Pggt1b^{fl/Δ}K* mice. (Scale bars, 100 μ m.)

cells in *Fntb*^{fl/Δ}*Pggt1b*^{fl/Δ}*KL* lungs clearly lacked both enzymes, as a large proportion of K-RAS in lung lysates was found in the cytosolic fraction. Also, immunochemical studies revealed that some cells were positive for both prelamin A and np-RAP1A. It is intriguing that some cells in the lung were apparently viable despite the absence of both FTase and GGTase-I. However, our genetic approach does not allow us to address the impact of FTase and GGTase-I deficiency in every lung cell (such as lung stem cells), and we cannot rule out the possibility that a more widespread inactivation of these enzymes would be toxic.

In summary, our findings support the idea that farnesylation is essential for H-RAS membrane association, HDJ2 prenylation, and fibroblast proliferation in vitro. In mice harboring a mutationally activated form of K-RAS in the lung, blocking protein farnesylation retarded tumor growth and improved survival. Our results also support the idea that simultaneous inhibition of FTase and GGTase-I could be therapeutically useful. Finally, the experimental approach described here should be useful for dissecting the in vivo importance of protein farnesylation and geranylgeranylation in other cell types in a variety of diseases.

- Lane KT, Beese LS (2006) Lipid posttranslational modifications. Structural biology of protein farnesyltransferase and geranylgeranyltransferase type I. *J Lipid Res* 47: 681–699.
- Seabra MC, Reiss Y, Casey PJ, Brown MS, Goldstein JL (1991) Protein farnesyltransferase and geranylgeranyltransferase share a common α subunit. *Cell* 65:429–434.
- Casey PJ, Seabra MC (1996) Protein prenyltransferases. *J Biol Chem* 271:5289–5292.
- Kato K, et al. (1992) Isoprenoid addition to Ras protein is the critical modification for its membrane association and transforming activity. *Proc Natl Acad Sci USA* 89:6403–6407.
- Bos JL (1989) *ras* oncogenes in human cancer: A review. *Cancer Res* 49:4682–4689.
- Basso AD, Kirschmeier P, Bishop WR (2006) Lipid posttranslational modifications. Farnesyl transferase inhibitors. *J Lipid Res* 47:15–31.
- Kohl NE, et al. (1995) Inhibition of farnesyltransferase induces regression of mammary and salivary carcinomas in *ras* transgenic mice. *Nat Med* 1:792–797.
- Omer CA, et al. (2000) Mouse mammary tumor virus-Ki-rasB transgenic mice develop mammary carcinomas that can be growth-inhibited by a farnesyl:protein transferase inhibitor. *Cancer Res* 60:2680–2688.
- Sepp-Lorenzino L, et al. (1995) A peptidomimetic inhibitor of farnesyl:protein transferase blocks the anchorage-dependent and -independent growth of human tumor cell lines. *Cancer Res* 55:5302–5309.
- Sebti SM, Hamilton AD (2000) Farnesyltransferase and geranylgeranyltransferase I inhibitors and cancer therapy: Lessons from mechanism and bench-to bedside translational studies. *Oncogene* 19:6584–6593.
- Sebti SM, Der CJ (2003) Searching for the elusive targets of farnesyltransferase inhibitors. *Nat Rev Cancer* 3:945–951.
- End DW, et al. (2001) Characterization of the antitumor effects of the selective farnesyl protein transferase inhibitor R115777 in vivo and in vitro. *Cancer Res* 61:131–137.
- Liu M, et al. (1998) Antitumor activity of SCH 66336, an orally bioavailable tricyclic inhibitor of farnesyl protein transferase, in human tumor xenograft models and *wap-ras* transgenic mice. *Cancer Res* 58:4947–4956.
- Rose WC, et al. (2001) Preclinical antitumor activity of BMS-214662, a highly apoptotic and novel farnesyltransferase inhibitor. *Cancer Res* 61:7507–7517.
- Hunt JT, et al. (2000) Discovery of (R)-7-cyano-2,3,4,5-tetrahydro-1-(1H-imidazol-4-ylmethyl)-3-(phenylmethyl)-4-(2-thienylsulfonyl)-1H-1,4-benzodiazepine (BMS-214662), a farnesyltransferase inhibitor with potent preclinical antitumor activity. *J Med Chem* 43: 3587–3595.
- Mijimolle N, et al. (2005) Protein farnesyltransferase in embryogenesis, adult homeostasis, and tumor development. *Cancer Cell* 7:313–324.
- Lerner EC, et al. (1995) Ras CAAX peptidomimetic FTI-277 selectively blocks oncogenic Ras signaling by inducing cytoplasmic accumulation of inactive Ras-Raf complexes. *J Biol Chem* 270:26802–26806.
- Willumsen BM, Christensen A, Hubbert NL, Papageorge AG, Lowy DR (1984) The p21 ras C-terminus is required for transformation and membrane association. *Nature* 310: 583–586.
- Ashar HR, et al. (2000) Farnesyl transferase inhibitors block the farnesylation of CENP-E and CENP-F and alter the association of CENP-E with the microtubules. *J Biol Chem* 275:30451–30457.
- Crespo NC, Ohkanda J, Yen TJ, Hamilton AD, Sebti SM (2001) The farnesyltransferase inhibitor, FTI-2153, blocks bipolar spindle formation and chromosome alignment and causes prometaphase accumulation during mitosis of human lung cancer cells. *J Biol Chem* 276:16161–16167.
- Nagasu T, Yoshimatsu K, Rowell C, Lewis MD, Garcia AM (1995) Inhibition of human tumor xenograft growth by treatment with the farnesyl transferase inhibitor B956. *Cancer Res* 55:5310–5314.

Materials and Methods

A Conditional Knockout Allele for *Fntb*. A 2.2-kb fragment spanning promoter sequences, exon 1, and parts of intron 1 was amplified by PCR from the genomic DNA of strain 129/OlaHsd embryonic stem (ES) cells. The fragment was cloned into *pNB1*, which contains a polylinker flanked by *loxP* sites. The floxed fragment was excised and cloned into *pKS/loxPNTmod* (41) upstream of a floxed *neo* cassette. Finally, 5'- and 3'-flanking arms were amplified by PCR and cloned upstream and downstream, respectively, of the floxed exon 1 fragment and *neo* cassette. The gene-targeting vector was electroporated into 129/OlaHsd ES cells, and targeted clones (identified by Southern blotting with flanking probes) were used to produce germline-transmitting chimeric mice. A detailed description of all other methods appears in *SI Materials and Methods*.

ACKNOWLEDGMENTS. We thank Drs. Hans Nordlinder and Aziz Hussein for assistance with lung histopathology. This study was supported by a Starting Investigator Grant from the European Research Council; by grants from the Swedish Cancer Society, the Swedish Medical Research Council, the Swedish Children's Cancer Fund, and Västra Götalandsregionen (to M.O.B.); by the Medical Society of Gothenburg and the Foundations of Assar Gabrielsson, Serena Ehrenströms, and Konrad and Helfrid Johansson (to M.L.); and by National Institutes of Health Grants AR050200 and HL76839 and an Ellison Medical Foundation Senior Scholar Award (to S.G.Y.). The funders had no role in study design, data collection and analysis, decision to publish, or preparation of the manuscript.

- Yang SH, et al. (2009) Caution! Analyze transcripts from conditional knockout alleles. *Transgenic Res* 18:483–489.
- James G, Goldstein JL, Brown MS (1996) Resistance of K-RasB^{V12} proteins to farnesyltransferase inhibitors in Rat1 cells. *Proc Natl Acad Sci USA* 93:4454–4458.
- Whyte DB, et al. (1997) K- and N-Ras are geranylgeranylated in cells treated with farnesyl protein transferase inhibitors. *J Biol Chem* 272:14459–14464.
- Rowell CA, Kowalczyk JJ, Lewis MD, Garcia AM (1997) Direct demonstration of geranylgeranylation and farnesylation of Ki-Ras in vivo. *J Biol Chem* 272:14093–14097.
- El Oualid F, Cohen LH, van der Marel GA, Overhand M (2006) Inhibitors of protein: Geranylgeranyl transferases. *Curr Med Chem* 13:2385–2427.
- Sun J, Qian Y, Hamilton AD, Sebti SM (1998) Both farnesyltransferase and geranylgeranyltransferase I inhibitors are required for inhibition of oncogenic K-Ras prenylation but each alone is sufficient to suppress human tumor growth in nude mouse xenografts. *Oncogene* 16:1467–1473.
- Sun J, et al. (1999) Antitumor efficacy of a novel class of non-thiol-containing peptidomimetic inhibitors of farnesyltransferase and geranylgeranyltransferase I: Combination therapy with the cytotoxic agents cisplatin, Taxol, and gemcitabine. *Cancer Res* 59: 4919–4926.
- Sun J, et al. (2003) Geranylgeranyltransferase I inhibitor GGTI-2154 induces breast carcinoma apoptosis and tumor regression in H-Ras transgenic mice. *Cancer Res* 63: 8922–8929.
- Peterson YK, Kelly P, Weinbaum CA, Casey PJ (2006) A novel protein geranylgeranyltransferase-I inhibitor with high potency, selectivity, and cellular activity. *J Biol Chem* 281:12445–12450.
- Watanabe M, et al. (2008) Inhibitors of protein geranylgeranyltransferase I and Rab geranylgeranyltransferase identified from a library of allenolate-derived compounds. *J Biol Chem* 283:9571–9579.
- Sjogren A-KM, et al. (2007) GGTase-I deficiency reduces tumor formation and improves survival in mice with K-RAS-induced lung cancer. *J Clin Invest* 117:1294–1304.
- Lobell RB, et al. (2001) Evaluation of farnesyl:protein transferase and geranylgeranyl: protein transferase inhibitor combinations in preclinical models. *Cancer Res* 61: 8758–8768.
- deSolms SJ, et al. (2003) Dual protein farnesyltransferase-geranylgeranyltransferase-I inhibitors as potential cancer chemotherapeutic agents. *J Med Chem* 46:2973–2984.
- Di Paolo A, et al. (2001) Inhibition of protein farnesylation enhances the chemotherapeutic efficacy of the novel geranylgeranyltransferase inhibitor BAL9611 in human colon cancer cells. *Br J Cancer* 84:1535–1543.
- Lakso M, et al. (1996) Efficient in vivo manipulation of mouse genomic sequences at the zygote stage. *Proc Natl Acad Sci USA* 93:5860–5865.
- Schwenk F, Baron U, Rajewsky K (1995) A *cre*-transgenic mouse strain for the ubiquitous deletion of *loxP*-flanked gene segments including deletion in germ cells. *Nucleic Acids Res* 23:5080–5081.
- Jackson EL, et al. (2001) Analysis of lung tumor initiation and progression using conditional expression of oncogenic *K-ras*. *Genes Dev* 15:3243–3248.
- Adjei AA, et al. (2000) A phase I trial of the farnesyl transferase inhibitor SCH66336: Evidence for biological and clinical activity. *Cancer Res* 60:1871–1877.
- Lebowitz PF, Prendergast GC (1998) Non-Ras targets of farnesyltransferase inhibitors: Focus on Rho. *Oncogene* 17 (11 Reviews):1439–1445.
- Hanks M, Wurst W, Anson-Cartwright L, Auerbach AB, Joyner AL (1995) Rescue of the *En-1* mutant phenotype by replacement of *En-1* with *En-2*. *Science* 269:679–682.

Supporting Information

Liu et al. 10.1073/pnas.0908396107

SI Materials and Methods

Mouse Breeding. *Fntb*^{fl/fl} mice were bred with EIIa-*Cre* mice to excise the floxed *neo* cassette (without excising the floxed exon 1). Mice homozygous for this “delta *neo*” *Fntb*^{fl} allele were mated with deleter-*Cre* transgenic mice to excise the floxed exon 1 and generate mice carrying a germline knockout allele (*Fntb*^Δ). To determine the impact of *Fntb* deficiency on K-RAS-induced lung cancer, we bred *Fntb*^{fl/Δ} mice carrying a single *Kras*^{2^{LSL}} allele (*K*) (1). The expression of *Cre* in those mice with a lysozyme M-*Cre* allele (*L*) (2) simultaneously switched on the expression of K-RAS^{G12D} and inactivated *Fntb* expression in the lung. Littermate *Fntb*^{fl/+}*KL* mice were used as positive controls for the development of tumors, and *Fntb*^{fl/Δ} and *Fntb*^{fl/+} mice harboring the *K* or *L* allele, but not both, served as negative controls. To determine the effect of inactivating both *Fntb* and *Pggt1b* on K-RAS-induced lung cancer, we bred *Fntb*^{fl/Δ}*Pggt1b*^{fl/Δ}*KL* and control mice. The *Pggt1b*^{fl} allele has been described (3). Mice had a mixed genetic background (129OlaHsd and C57BL/6). All experiments were approved by the Animal Research Ethics Committee in Gothenburg.

Genotyping and Quantification of *Cre* Recombination of Floxed Alleles. The *Fntb*⁺ and *Fntb*^{fl} alleles were genotyped by PCR amplification of genomic DNA with forward primer 5'-GGTGGATGGGAAATTGGG-3' and reverse primer 5'-AGCAGCCACCTGGAGACTTA-3' and yielded 252- and 320-bp fragments, respectively; the *Fntb*^Δ allele was amplified with forward primer 5'-GTGAGCCTGTATTACTGTGCC-3' and reverse primer 5'-CCTGGTCTACGGAGTAGTTC-3' and yielded an 800-bp fragment. The *K*^{LSL}, *K*^{G12D}, *Pggt1b*^{fl}, and *L* alleles were genotyped as described (3). The impact of *Cre* recombination on *Fntb* transcripts was assessed by PCR amplification of sequences spanning *Fntb* exons 1–6 (forward primer 5'-TACAGCGCTCGAGCTCTCC-3' and reverse primer 5'-TCGGGTTGCTTTAGGG AGT A-3'; product size, 588 bp) and exon 3–5 sequences (5'-AGAGGCCTTCGACA ACTGA-3' and 5'-CATTGACGGCTGCATA AGTG-3'; product size, 214 bp) on cDNA synthesized from total RNA with the iScript cDNA Synthesis Kit (Bio-Rad). To quantify the *Cre*-induced inactivation of the *Fntb*^{fl} allele, we performed real-time quantitative PCR with Power SYBR Green PCR Master Mix on an ABI Prism 7900HT system (Applied Biosystems), using genomic DNA from lung tissue and tumors. The primers, localized within the floxed segment, were 5'-CAATTAGGCGAGAGCGAAAC-3' and 5'-GCAGGAGATCAGCTTTCTGG-3'. The percentage of genomic DNA with an inactivated *Fntb* allele was calculated using a reference gene (*Rce1*, amplified with primers 5'-CGAGTAAATCTGTGGGAGAGG-3' and 5'-CGGTGCAATAACTTGGTTTC-3'). Primers used to quantify the inactivation of the *Pggt1b*^{fl} allele and the STOP cassette in the *K*^{LSL} allele were described previously (3).

Isolation of Embryonic Fibroblasts and *Cre*-Adenovirus Infection. Primary fibroblasts were isolated from embryos 13.5 days post coitum, and experiments were performed with passage of 2–4 cells. One million cells were seeded in 100-mm dishes and incubated with 10⁸ pfu/mL of a *Cre*-adenovirus (Ad5CMV*Cre*, designated *adCre*; University of Iowa, Iowa City, IA) or a control β-gal-adenovirus (Ad5CMVnt*LacZ*, designated *adβgal*; University of Iowa) for 24 h in 5 mL of medium. In some experiments, *Fntb*^{fl/Δ} cells were incubated with *adCre* and a GGTI (10 μM, GGTI-298; Sigma) for 4 days.

Subcellular Fractionation and Western Blotting. Membrane and cytosolic fractions of fibroblasts were isolated by centrifugation at 100,000 × *g* as described (4). Membrane and cytosolic fractions of

lung lysates were isolated with the Qproteome Cell Compartment Kit (37502; Qiagen). For western blotting, equal amounts of protein from subcellular fractions or total cell extracts from fibroblasts or tissues were size-fractionated on 10–20% or 18% SDS/PAGE gels (Criterion; Bio-Rad). The proteins were transferred to nitrocellulose membranes and incubated with antibodies recognizing H-RAS (sc-520), N-RAS (sc-31), nonprenylated (np) RAPIA (sc-1482) (Santa Cruz Biotechnology), HDJ2 (MS-225-P; Lab Vision), K-RAS (OP24; Calbiochem), prelamin A (5), phosphorylated ERK1/2 (9106; Cell Signaling), total ERK1/2 (9102; Cell Signaling), or actin (A2066; Sigma). Protein bands were visualized with a horseradish peroxidase-conjugated secondary antibody (sc-2354; Santa Cruz Biotechnology) (NA931, NA934; GE Healthcare Life Sciences) and the ECL Western Blotting System (GE Healthcare). Densitometry of protein bands was analyzed with Quantity One 4.4.0 software (Bio-Rad).

Cell Proliferation. Cells (2 × 10³) were seeded in duplicate in 12-well plates and incubated in serum-free medium overnight. The medium was then replaced with medium containing 10% serum and, at the indicated times, the cells were trypsinized and counted.

Histological Analyses and Immunofluorescence. For routine histology, paraformaldehyde-fixed tissues were sectioned (4 μm) and stained with hematoxylin and eosin. For immunofluorescence analyses, lung tissue was embedded in OCT (Sakura Finetek) and frozen at –80°C. Cryosections (5-μm) were incubated with antibodies recognizing prelamin A [a rabbit antiserum (5) or a new rat monoclonal antibody], np-RAPIA (sc-1482; Santa Cruz Biotechnology), SP-C (AB3786; Millipore), or Ki-67 (SP6; Thermo Fisher Scientific) overnight at 4 °C. Secondary antibodies were conjugated with Cy3 (Jackson ImmunoResearch), Alexa Fluor 647 (Molecular Probes, Invitrogen), or Alexa Fluor 488 (Molecular Probes, Invitrogen). The secondary antibodies were incubated for 1 h. Sections were mounted and stained with Prolong-Gold Antifade reagent with DAPI (Molecular Probes, Invitrogen). The slides were then analyzed with a Leica TCS SP5 confocal microscope (Leica Microsystems) and LAS Advanced Fluorescence software (version 2.0.2; Leica Microsystems). Lung sections from *Zmpste24*^{–/–} mice (6) were used as a positive control for prelamin A staining.

Inhalation of *adCre*. The *adCre* was prepared as a calcium-phosphate coprecipitate as described (7) and incubated for 20 min at room temperature. Mice (5–9 weeks old) were allowed to inhale *adCre* (5 × 10⁷ pfu in a volume of 125 μL, administered in two 62.5-μL doses) under general anesthesia (1).

Scoring of Lung Tumor Number and Lesion Area. Lungs were inflated and fixed with paraformaldehyde, and each lobe was embedded in paraffin. Three sections (at 200-μm intervals) of lobes 1, 3, and 5 were stained with hematoxylin and eosin. Tumor number was assessed by counting tumors under the microscope at 10× magnification. To quantify lung tumor area, the third (middle) section of lobe 3 from each mouse was analyzed with Biopix iQ software (version 2.1.3; Biopix).

Cell-Cycle Analysis. Fibroblasts at 75% confluency were trypsinized, washed with PBS, and fixed in 70% ethanol. The cells were incubated with propidium iodide and RNase A for 30 min at 37 °C and analyzed in a FACScan flow cytometer with CellQuest Pro software (version 4.0.2; Becton Dickinson).

Apoptosis Analysis. One million *Fntb*^{fl/fl}*Pggt1b*^{fl/fl} cells were seeded in 100-mm dishes and infected with *adβgal* or *adCre* for 4 days.

Apoptosis was then detected with the Annexin V-EGFP Apoptosis Kit (K104-100; Biovision). Apoptosis in tissues was detected by TUNEL staining (ApopTag Fluorescein In Situ Apoptosis Detection Kit; s7110; Millipore) and by immunohistochemistry with an antibody recognizing cleaved caspase 3 (9661; Cell Signaling).

Transfection of Fibroblasts with a Myristoylated H-RAS (Q61L) Plasmid. A plasmid encoding human H-RAS (Q61L) with an 11-amino acid N-terminal myristoylation signal (8) was transfected into

immortalized *Fntb^{fl/fl}Pggt1b^{fl/fl}* fibroblasts with FuGENE 6 reagent (Roche Diagnostics). Cells were then incubated with *adβgal* or *adCre* and photographed 4 days later.

Statistics. Data are plotted as mean and standard error of the mean. Differences in cellular proliferation, density of protein bands on western blots, lung weight, tumor number, and lesion area were determined with Student's *t* test or one-way ANOVA with Tukey's posthoc test; survival was assessed with the log-rank test.

1. Jackson EL, et al. (2001) Analysis of lung tumor initiation and progression using conditional expression of oncogenic *K-ras*. *Genes Dev* 15:3243–3248.
2. Clausen BE, Burkhardt C, Reith W, Renkawitz R, Förster I (1999) Conditional gene targeting in macrophages and granulocytes using LysMcre mice. *Transgenic Res* 8: 265–277.
3. Sjogren A-KM, et al. (2007) GGTase-I deficiency reduces tumor formation and improves survival in mice with K-RAS-induced lung cancer. *J Clin Invest* 117:1294–1304.
4. Bergo MO, et al. (2004) Inactivation of *lcm1* inhibits transformation by oncogenic K-Ras and B-Raf. *J Clin Invest* 113:539–550.
5. Fong LG, et al. (2006) Prelamin A and lamin A appear to be dispensable in the nuclear lamina. *J Clin Invest* 116:743–752.
6. Bergo MO, et al. (2002) *Zmpste24* deficiency in mice causes spontaneous bone fractures, muscle weakness, and a prelamin A processing defect. *Proc Natl Acad Sci USA* 99:13049–13054.
7. Fasbender A, et al. (1998) Incorporation of adenovirus in calcium phosphate precipitates enhances gene transfer to airway epithelia in vitro and in vivo. *J Clin Invest* 102:184–193.
8. Winter-Vann AM, et al. (2003) Targeting Ras signaling through inhibition of carboxyl methylation: An unexpected property of methotrexate. *Proc Natl Acad Sci USA* 100: 6529–6534.

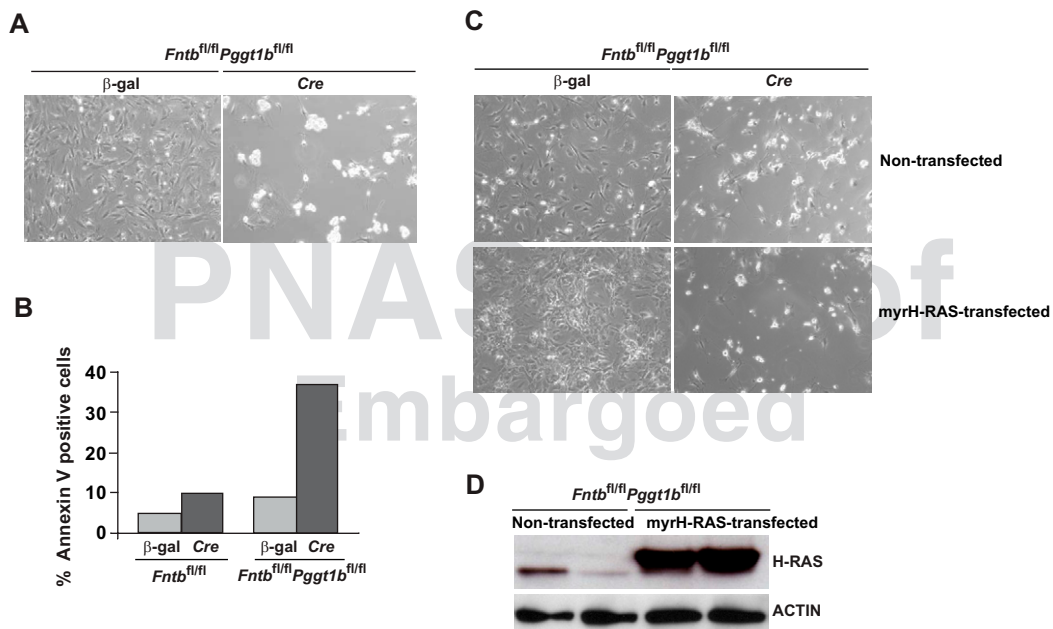


Fig. S1. Simultaneous inactivation of *Fntb* and *Pggt1b* in fibroblasts induces apoptosis. (A) Photographs of *Fntb^{fl/fl}Pggt1b^{fl/fl}* fibroblasts 4 days after incubation with *adβgal* or *adCre*. (B) Percent apoptotic cells in cultures of *Fntb^{fl/fl}* and *Fntb^{fl/fl}Pggt1b^{fl/fl}* cells 4 days after incubation with *adβgal* or *adCre*. Data are from one cell line. Similar results were obtained in two experiments with two cell lines of each genotype. (C) Photographs of H-RAS (Q61L)-transfected and untransfected *Fntb^{fl/fl}Pggt1b^{fl/fl}* fibroblasts 4 days after incubation with *adβgal* or *adCre*. (D) Western blots of extracts from *Fntb^{fl/fl}Pggt1b^{fl/fl}* fibroblasts showing expression of the myristoylated H-RAS (Q61L) construct. Actin was used as a loading control.

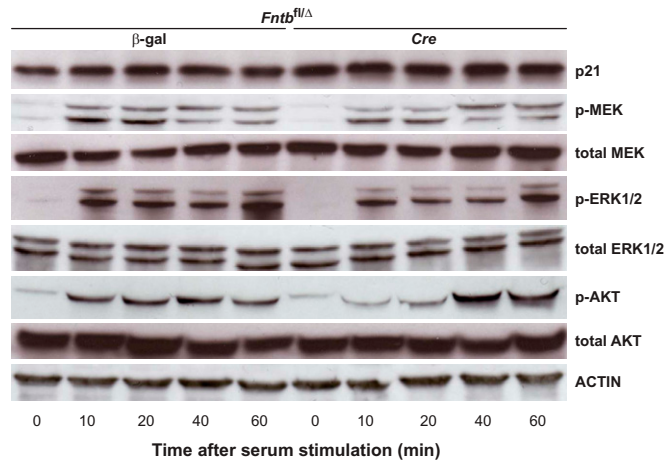


Fig. S2. Basal and serum-stimulated levels of p21^{CIP1} and phosphorylation of downstream RAS effectors. *Fntb^{fl/Δ}* cells (10^5) treated with *adβgal* or *adCre* were seeded on 60-mm dishes, incubated in serum-free medium overnight, and stimulated with medium containing 10% serum. Total cell extracts were harvested at various times and analyzed by western blotting with antibodies recognizing p21^{CIP1} (sc-6246; Santa Cruz Biotechnology), phosphorylated MEK (9121), total MEK (9122), phosphorylated ERK1/2 (9106), total ERK1/2 (9102), phosphorylated AKT^{Ser-473} (9271), and total AKT (9272) (Cell Signaling). Actin (A2066; Sigma) was used as a loading control.

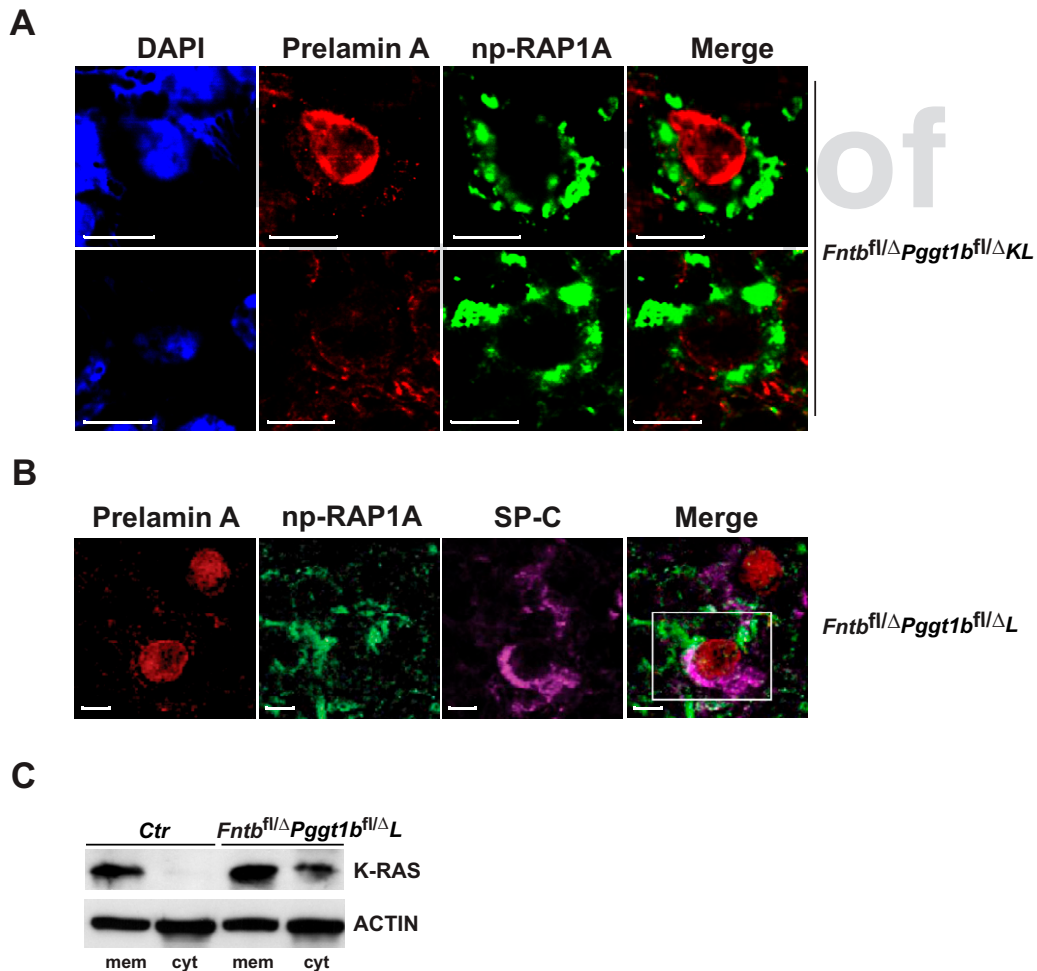


Fig. S3. Identification of cells expressing markers of absent FTase and GGTase-I activity. (A) Immunofluorescence confocal microscopy of lung sections from 3-week-old *Fntb^{fl/Δ}Pggt1b^{fl/Δ}KL* mice. Cells positive for both prelamin A (red, nuclear staining) and np-RAP1A (green, cytoplasmic staining) are seen in the upper panel; a cell positive for np-RAP1A but negative for prelamin A is seen in the lower panel. Nuclei are stained with DAPI (blue). (Scale bars, 10 μ m.) (B) Immunofluorescence confocal microscopy showing expression of prelamin A (red), np-RAP1A (green), and SP-C (purple) in the lung of a 3-week-old *Fntb^{fl/Δ}Pggt1b^{fl/Δ}L* mouse. Boxed: Cell positive for all three markers. (Scale bars, 10 μ m.) (C) Western blots showing the distribution of K-RAS in the membrane and cytosol fractions of lungs from control and *Fntb^{fl/Δ}Pggt1b^{fl/Δ}L* mice.

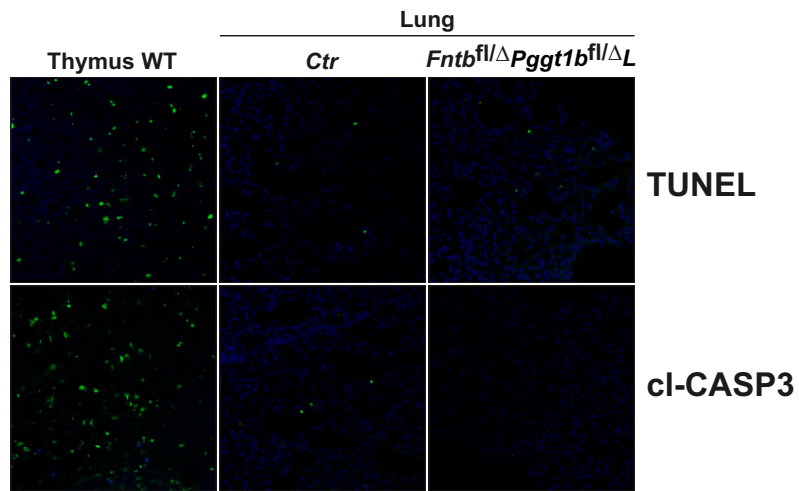


Fig. 54. No evidence of apoptosis in lungs of *Fntb^{fl/Δ}Pggt1b^{fl/ΔL}* mice. TUNEL and cleaved caspase 3 (cI-CASP3) staining in lungs of 3-week-old *Fntb^{fl/Δ}Pggt1b^{fl/ΔL}* and control mice. Sections of thymus from a 3-week-old wild-type mouse was used as a positive control.

PNAS proof
Embargoed